

Peter R. Ashton, Kenneth D. M. Harris, Benson M. Kariuki, Douglas Philp,*†
James M. A. Robison and Neil Spencer

School of Chemistry, University of Birmingham, Edgbaston, Birmingham, UK B15 2TT

Received (in Cambridge, UK) 31st May 2001, Accepted 1st August 2001

First published as an Advance Article on the web 16th October 2001

A diboradiazaromatic—2,7-di-*tert*-butyl-5,9-dihydroxy-5,9-dibora-4,10-diazapyrene-4,10-dium-5,9-diide— which is a structural analogue of isophthalic acid has been designed and synthesised. This compound is capable of spontaneous dehydration in solution to form linear oligoanhydrides. These oligoanhydrides can be readily hydrolysed to the starting diboradiazaromatic under appropriate conditions. This unusual reactivity is mirrored in the solid-state behaviour of 2,7-di-*tert*-butyl-5,9-dihydroxy-5,9-dibora-4,10-diazapyrene-4,10-dium-5,9-diide. A complex network of hydrogen bonds present in the solid-state structure of the borazaaromatic serve to facilitate a facile solid-state dehydration reaction, once again forming oligoanhydrides of molecular weight greater than 3000 Da.

Introduction

Solid-state organic reactivity continues to attract significant interest since its exploitation can provide enhanced rates of reactions as well as differing degrees of regio- and stereo-selectivity when compared to reactions performed in solution.¹ Solid-state organic reactions can occur between two solids, between a liquid and a solid or between a gas and a solid. However, it is transformations within crystals that are of particular interest to the supramolecular chemist, since molecular recognition may be exploited to control the structural and geometric arrangement of potentially reactive molecules within the solid-state, and hence, control their reactivity. In the past, investigations of organic solid-state transformations have mostly concentrated upon [2 + 2] photodimerisations, and examples utilising intermolecular interactions to align photo-reactive alkene^{2,3} and bisalkene⁴ compounds have been reported. Somewhat surprisingly, other types of organic solid-state transformations, especially bond forming reactions which proceed under thermal control, appear to have been studied much less extensively,⁵ and examples of the use of molecular recognition to facilitate and control such reactions are scarce.

Borazaaromatics are a class of compounds analogous to aromatic hydrocarbons, in which a C=C fragment has been replaced by an isoelectronic $^{-}B=N^{+}$ fragment. Although several borazaaromatics were synthesised in the 1950s and 1960s, their chemical properties were never investigated fully.⁶ Recently, we identified two important chemical characteristics of these compounds. Firstly, we recognised a structural similarity between the recognition properties of carboxylic acids and hydroxyborazaaromatics. Thus, the hydroxyborazaaromatic self-complementary hydrogen bonded dimer **2** is analogous to the carboxylic acid supramolecular synthon^{7,8} **1** (Fig. 1). Secondly, unlike carboxylic acids, which are relatively inert towards self-condensation to give anhydrides, hydroxyborazaaromatics readily undergo dehydration, in solution or the solid-state, to form the corresponding anhydride (Scheme 1). The first system studied⁹ in depth was 10-hydroxy-10-bora-9-azaphenanthren-9-ium-10-uide **4**, which is a structural analogue of phenanthrene and a recognition analogue of benzoic acid **3**. Compound **4** undergoes a solid-state transformation to form

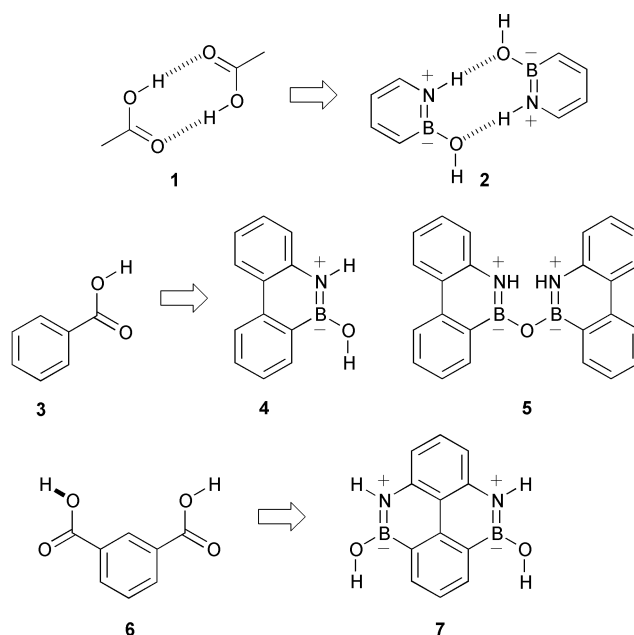
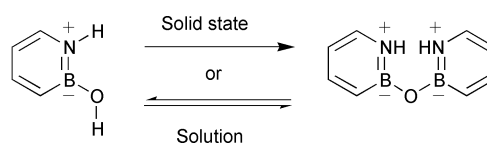


Fig. 1 The borazaaromatic supramolecular synthon **2** is structurally analogous to the carboxylic acid synthon **1**. Thus, carboxylic acids **3** and **6** share the same recognition properties as borazaaromatics **4** and **7** respectively.



Scheme 1 Hydroxyborazaaromatics are converted into the corresponding anhydride either in the solid-state (by heating) or in solution (by control of the solvent polarity). Non-polar solvents (e.g. $CHCl_3$, CH_2Cl_2 , benzene) favour the formation of the anhydride whereas polar solvents (e.g. acetone, CH_3CN , DMSO) favour the formation of the hydroxy compound.

the anhydride **5** irreversibly when a sample is heated at relatively low temperatures (100 °C, 1 h). In solution, the inter-conversion between **4** and **5** is under thermodynamic control. The mechanism for the conversion of **4** to **5** is presumed to involve nucleophilic attack of the hydroxy group of one molecule at the electrophilic boron centre of a second molecule.

† Present address: Centre for Biomolecular Sciences, School of Chemistry, University of St Andrews, North Haugh, St Andrews, Fife, UK KY16 9ST.

Although the charge representation of the $\text{B}=\text{N}^+$ bond suggests that the boron has a partial negative charge, the calculated electrostatic potential surface around the boron centre in **4** is actually positive, inferring that the $\text{N}\rightarrow\text{B}$ charge transfer π -bonding framework is outweighed by the $\text{B}\rightarrow\text{N}$ charge transfer σ -bonding framework. The enhanced reactivity of these hydroxyborazaaromatics, in comparison with carboxylic acids, reflects the modified reactivity of the electrophilic centre—the carbonyl carbon atom *vs.* the borazaaromatic boron atom.

Given that the $\text{R}_2(8)^{10}$ cyclic homodimer **1** formed by carboxylic acids has been used extensively in the design of organic solids, we recognised that the similarity between the recognition characteristics of motifs **1** and **2**, coupled with the modified electrophilic chemistry of motif **2**, could be exploited in the creation of chemical systems which are able to (a) participate in intermolecular recognition similar to that seen in molecular solids bearing carboxylic acid functionality and (b) possess the latent capability of a covalent bond formation reaction in the solid-state *via* self-condensation. The tendency for molecules bearing two or more carboxylic acid groups to form hydrogen bonded tapes and sheets in the solid-state, such as those seen in isophthalic acid^{11,12} and trimesic^{13,14} acid (benzene-1,3,5-tricarboxylic acid) derivatives, has been exploited in crystal engineering and solution-phase supramolecular chemistry. Therefore, in principle, replacement of the carboxylic acid recognition motif by a motif that shares the same recognition characteristics and has enhanced reactivity towards self-condensation, should lead to chemical systems capable of forming extended covalently bonded structures (*i.e.* polymers).

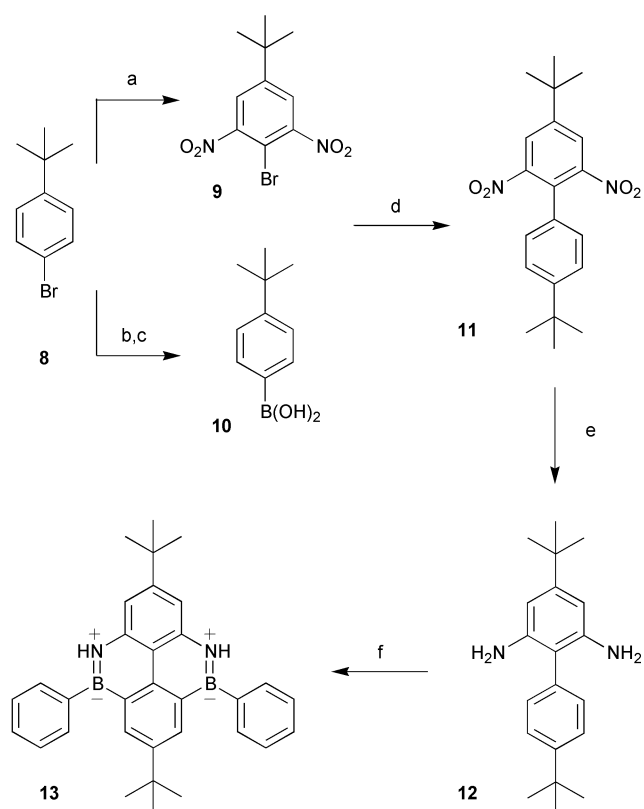
In this paper, we report the use of the electrophilic reactivity of a borazaaromatic analogue of isophthalic acid in the design of novel polymers which can be formed under equilibrium control in solution or non-reversibly *via* a solid-state transformation.

Results and discussion

The design of a borazaaromatic system which could mimic the recognition properties of a carboxylic acid such as isophthalic acid requires an aromatic skeleton in which two boron atoms are bonded to the same phenyl ring. Therefore, we selected a pyrene skeleton bearing two boron–nitrogen functionalities, representing a borazaaromatic that is practical both in terms of synthesis and aromatic stability. The dihydroxydiazadiborapyrene **7** is a structural analogue of isophthalic acid **6** and a *B*-phenyl substituted borazapyrene has been reported¹⁵ to possess a similar UV spectrum to pyrene itself.

However, the intended synthesis of **7** required the preparation of 2,6-dinitrophenyl as an intermediate—a compound which is known¹⁶ to have poor solubility in organic solvents. Assuming that **7** would have similar solubility properties to 2,6-dinitrophenyl, we decided to append *tert*-butyl groups to the aromatic skeleton in order to improve solubility. We anticipated that the addition of these groups at the 4 and 4' positions on the biphenyl scaffold should simplify the ^1H NMR spectrum such that all the aromatic resonances appear as singlets.

4-*tert*-Butylbromobenzene **8** was nitrated affording the dinitro compound **9** and was also converted to the corresponding boronic acid **10** (Scheme 2). Cross-coupling of **9** and **10** using standard Suzuki¹⁷ methodology followed by catalytic reduction yielded the 2,6-diaminobiphenyl derivative **12**. In order to ensure that the diamine was suitable for the synthesis of borazaaromatics, we reacted **12** with PhBCl_2 to give the *B,B'*-diphenyl substituted borazapyrene **13** which, by virtue of its non-polar character and relative chemical stability, can be separated and characterised with ease. Our initial attempt to synthesise the corresponding dihydroxydiboradiazapyrene **14** using the methodology¹⁸ applied to the synthesis of **4** (using BCl_3 as the source of boron) was unsuccessful. However, the



Scheme 2 Reagents and conditions: (a) Fuming HNO_3 , 0°C , 30 min then 50°C , 20 min, 53%; (b) Mg , Et_2O ; (c) $\text{B}(\text{OMe})_3$, Et_2O , -76°C , 30 min then warm to 25°C , 48% (over two steps); (d) $\text{Pd}(\text{PPh}_3)_4$, 1 M Na_2CO_3 , DME , EtOH , H_2O , 85°C , 5 h, 57%; (e) Pd/C , H_2 , EtOAc , RT, 24 h, 84%; (f) PhBCl_2 , xylene, 138°C , 90 min then AlCl_3 , 138°C , 19 h, 22%.

reaction of diamine **12** with a $\text{BHCl}_2\cdot\text{Me}_2\text{S}$ complex afforded **14** (isolated as a mixture of oligomers **15**) in an estimated 72% yield.

Our initial attempts to grow crystals of **14** were unsuccessful, although, fortuitously, when a solution of **14–15** in CH_3OH was left to stand overnight, crystals of the dimethoxy ester **16** suitable for single crystal X-ray diffraction were formed; more concentrated methanolic solutions were found to produce a precipitate almost immediately after the preparation of the solution. The reaction of **14** with methanol provided further evidence that the boron centres in this diboradiazaromatic would be susceptible to nucleophilic attack in a similar manner to the electrophilic boron centre in **4**.

Single crystal X-ray diffraction studies were performed on these crystals of **16** for two purposes. Firstly, we wanted to confirm the molecular structure of **16** and thus, by implication, to establish the molecular structure of **14**. Secondly, in principle, it is possible for **16** to participate in hydrogen bonded ribbons (analogous to those observed in the solid-state structures of isophthalic acid and its derivatives) using motif **17**, provided the O–Me bond lies *anti* to the N–H bond. However, in the crystal structure¹⁹ of **16** (Fig. 2), all the molecules of **16** have the O–Me bond lying *syn* with respect to the N–H bond. The preference for this *syn* conformation, however, was confirmed by *ab initio* calculations on the model system, **18**. The $(\text{Ar})\text{C–B–O}$ bond angle of the optimised HF/6-31G(d,p) geometry of the *anti* conformer is somewhat strained (130.8°) by the proximity of the methyl hydrogens to the aromatic hydrogens at the 6- and 8-positions, *ortho* to the BOMe group ($d_{\text{H}\dots\text{H}} = 2.26 \text{ \AA}$). The *syn* conformer has the methyl group in close proximity to the NH hydrogen, but the steric hindrance is reduced ($d_{\text{H}\dots\text{H}} = 2.47 \text{ \AA}$) and thus the $(\text{Ar})\text{C–B–O}$ bond angle is less strained (123.6°). Accordingly, the energy of the *syn* conformer is estimated to be over 24 kJ mol^{-1} less than that for the

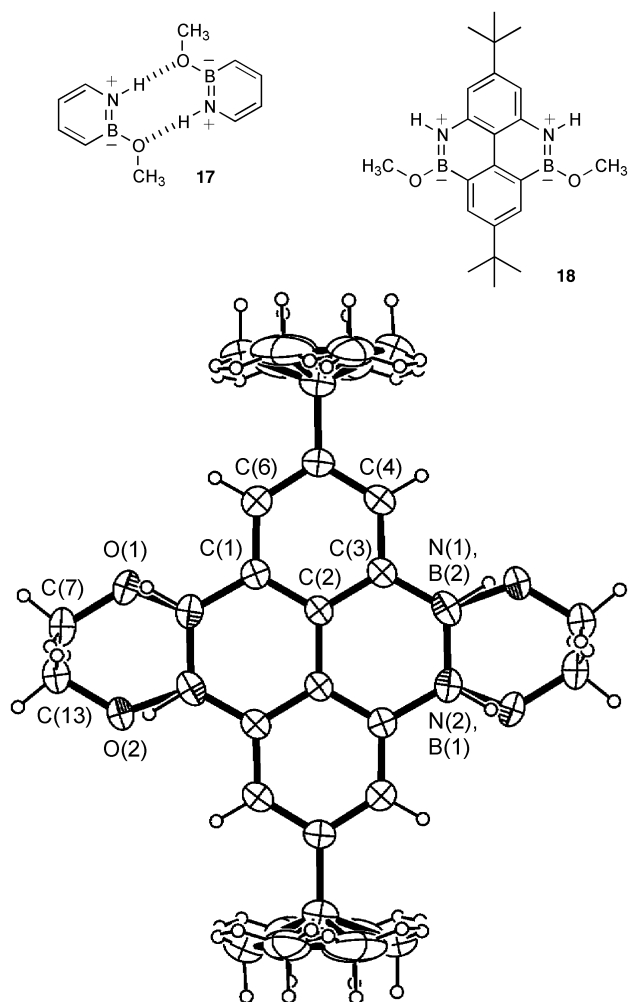


Fig. 2 ORTEP diagram of one of the disordered molecules of **16** in its crystal structure. Thermal ellipsoids are shown at the 30% probability level.

anti conformer. The crystal structure of **16** contains different types of disorder (see Fig. 2). Firstly, the methyl groups of the two *tert*-butyl substituents are disordered between two orientations (related by rotation around the C–C(CH₃)₃ bond). Secondly, the whole molecule is disordered between two molecular orientations (which can be regarded as being related by rotation about a 2-fold axis passing through the midpoints of the two B–N bonds). The two molecular orientations have equal populations, with the B atoms of one molecular orientation and the N atoms of the other molecular orientation occupying the same sites. From the crystal structure, we cannot assess whether the two molecular orientations represent two different ordered domains, or whether there is a uniform distribution of the two disordered molecular orientations throughout the crystal.

The dihydroxydiboradiazaromatic was initially isolated in a pure form by precipitation of the oligomer **15** by addition of hexane to a solution of a mixture of **14** and **15** in xylene. ¹H NMR analysis²⁰ in *d*₆-acetone (Fig. 3) shows that the oligoanhydride **15** hydrolyses to **14** over a period of one day, whereas the ¹H NMR spectrum of the same sample in a relatively non-polar solvent, CDCl₃, shows an equilibrium mixture of **14** and **15**. These observations confirm that the reversible electrophilic solution-phase reactivity seen in other borazaaromatics (Scheme 1) is also exhibited by the borazapyrene analogue; thus, the oligomer formation is under thermodynamic control. The equilibrium between **14** and **15** can be driven to give **14** by hydrolysis in polar solvents (such as acetone or DMSO) or the equilibrium can be shifted towards the side of **15** by spontaneous dehydration in a non-polar solvent (such as CHCl₃ or

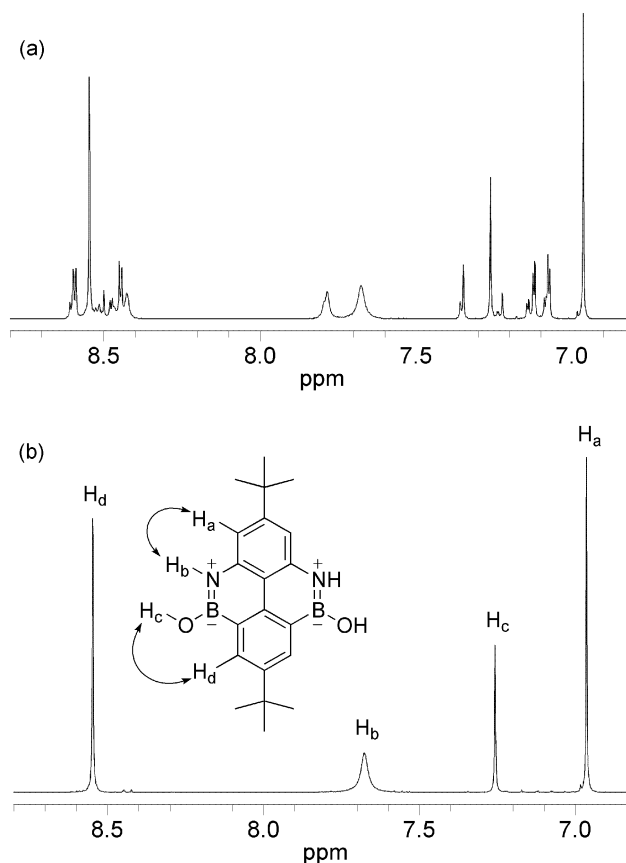


Fig. 3 (a) 300 MHz ¹H NMR spectrum of **14–15** in *d*₆-acetone solution recorded 1 hour after the solution was prepared. (b) The ¹H NMR spectrum of the same sample 24 hours later showing resonances for **14** only. The double-headed arrows represent NOEs which are observed in the 500 MHz ¹H NMR spectrum recorded of **14** in *d*₆-acetone solution at 30 °C.

hexane). Obviously, the concentration of water is critical in mediating the rate of hydrolysis. For example, the addition of a large excess of D₂O to a solution of **15** in *d*₆-acetone resulted in complete hydrolysis to **14** within a matter of minutes.

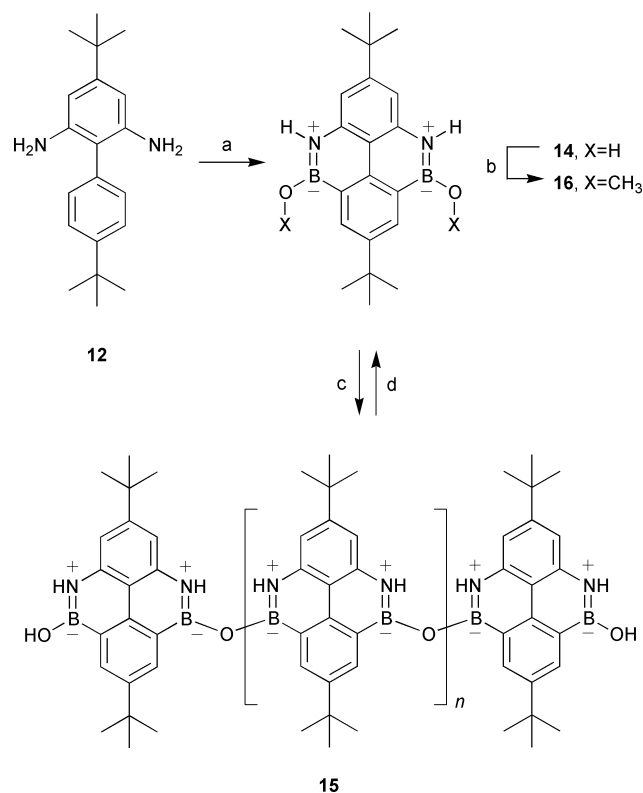
In order to investigate the effect of solvent (*i.e.* polar vs. non-polar) and the presence of water upon the length of the oligomer chain of **15** (represented by the value of *n*, Scheme 3) MALDI-TOF spectra were recorded for solutions of **14** and **15** in acetone and CHCl₃ in the presence and absence of 4 Å molecular sieves.

In the MALDI-TOF spectrum of a dilute solution of **14–15** in CHCl₃ (*ca.* 3 mM), the molecular ion [**14**⁺] is by far the largest peak (Table 1, entry A). However, peaks which could be assigned as oligoanhydrides **15** (*n* = 0, 1 and 2) could also be identified. We attribute the lack of larger oligomers to the presence of water in the CHCl₃ shifting the equilibrium to the hydrated compound **14**. Therefore, activated 4 Å molecular sieves were added to the CHCl₃ solution and the spectrum was re-recorded after two weeks. Oligomers as large as *n* = 7 were then observed (Fig. 4 and Table 1, entry B), suggesting that the removal of water by the molecular sieves shifts the equilibrium towards anhydride formation (*i.e.* **15**). It must be noted that the MALDI-TOF spectra do not provide a quantitative measure of the proportions of the oligomers present in the solution phase since the intensity of larger mass peaks is extremely sensitive to the power of the desorption laser; in the spectrum of the same sample recorded using a more powerful laser setting, the peaks representing the larger oligomers became more intense at the expense of a noisier background. However, peaks that could be assigned to oligomers with more than 10 repeat units (*i.e.* *n* > 8) were not obtained in any spectrum. Interestingly, only linear oligomers are observed (*i.e.* all the mass peaks correspond to

Table 1 Analysis of MALDI-TOF data

	% Area with respect to 14				
	A ^a	B	C	D	E
14	100	100	100	100	100
15 , where $n =$					
0	16	28	—	7	94
1	7	11	—	trace	54
2	trace	6	—	—	28
3	—	4	—	—	15
4	—	3	—	—	8
5	—	2	—	—	6
6	—	1	—	—	3
7	—	<1	—	—	1

^a **A** Solution in chloroform. **B** Solution in chloroform dried over 4 Å molecular sieves. **C** Solution of **14** in acetone. **D** Solution of **14** in acetone dried over 4 Å molecular sieves. **E** Crystal of [**14**₂·CH₃COCH₃] that has been heated at 160 °C for 5 hours.



Scheme 3 Reagents and conditions: (a) [BHCl₂·Me₂S], xylene, 138 °C, 2 h (Me₂S removed *in vacuo*) then AlCl₃, 20 h, 72%; (b) MeOH; (c) 4 Å molecular sieves, CHCl₃ or similar non-polar solvent; (d) H₂O and acetone or similar polar solvent.

oligomers with two terminal hydroxy groups), whereas cyclic oligomers would have 18 mass units less due to the loss of an extra water molecule in the cyclisation step.

In order to confirm that the larger oligomer peaks are not artifacts (for example arising from the aggregation of smaller oligomers upon ionisation), the MALDI-TOF spectrum was also obtained for a solution of **14** in acetone. The resulting spectrum had a peak corresponding to **14**, with no oligomers (**15**, $n \geq 0$) detected (Table 1, entry C). In contrast to the behaviour of the CHCl₃ solution, the presence of molecular sieves had little effect on the formation of oligomers. Two weeks after the addition of molecular sieves, the MALDI-TOF spectrum again showed that the peak corresponding to **14** was predominant (Table 1, entry D) and showed only a small increase (to 7% relative intensity) of the peak corresponding to the anhydride dimer (**15**, $n = 0$).

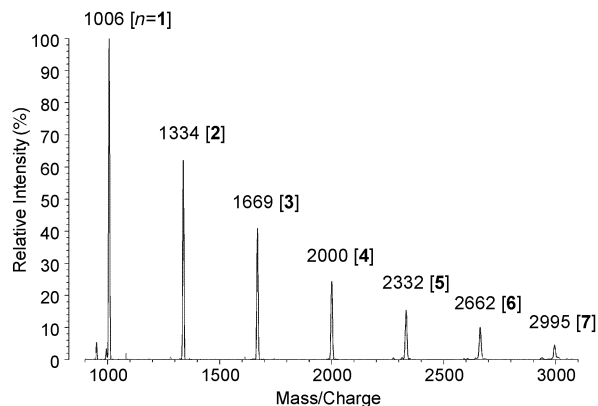


Fig. 4 Partial MALDI-TOF mass spectrum of borazapyrene oligomers **15** (where $n = 1$ to 7) obtained from a solution of **14**–**15** in dry CHCl₃.

These observations demonstrate unambiguously that in non-polar solvents such as CHCl₃, the solution equilibrium between **14** and **15** can be shifted in favour of **15** by the removal of water using very mild dehydrating agents (*i.e.* molecular sieves). However, it appears that in polar solvents, such as acetone and DMSO, the equilibrium lies far on the side of **14** and, thus, the reaction proceeds in one direction (hydrolysis of **15** to **14**).

Single crystals of a 2 : 1 complex of **14** and acetone suitable for single crystal X-ray diffraction studies were grown (following many attempts using different crystallisation techniques) by slow diffusion of hexane into a solution of **14** in an acetone–hexane mixture. Crystallisation from a variety of other solvent mixtures yielded only fine powders, emphasising the role of acetone in the formation of large single crystals. In the crystal structure²¹ of [**14**₂·acetone] (Fig. 5) molecules of **14** are arranged in a complex hydrogen bonding network of O–H···O and N–H···O interactions. Although this hydrogen bonding arrangement does not include the cyclic dimer motif **2**, the (B)O–H···O(B) and N–H···O(B) interactions bring the recognition sites, and thus the boron reaction centres, into close proximity. Fig. 5a demonstrates how the recognition sites 1 and 2 are linked together by O–H···O hydrogen bonds to the hydroxy group of recognition site 3 to form a chain of molecules running along the crystallographic *c* axis. Recognition site 4 is not part of the chain, although it does participate in N–H···O and O–H···O hydrogen bonds with the constituent hydroxy groups of the chain.

This hydrogen bonding network contains a number of cooperative and polarising interactions²² (Fig. 5b). The hydroxy oxygen of recognition site 3 accepts two hydrogen bonds (N–H···O from site 4 and O–H···O from site 1) thus making the hydroxy group an enhanced hydrogen bond donor. The hydroxy group of recognition site 2 participates in an O–H···O=C hydrogen bond with an acetone molecule, thus making it an enhanced hydrogen bond acceptor. The O–H···O hydrogen bond between the enhanced donor and acceptor is somewhat shorter ($d_{H\cdots O} = 1.76$ Å, O–H···O angle 170.5°) than the other O–H···O interactions in the structure. Indeed, all the O–H···O(H) distances lie within a range (1.76–1.90 Å) which is slightly shorter than the O–H···O(H) distance (1.92 Å) observed in the structure of **4**, emphasising the cooperative nature of the interactions in [**14**₂·acetone].

In hindsight, the absence of the predicted recognition motif **2** is readily rationalised. The presence of the *tert*-butyl groups on the aromatic skeleton disrupts close packing arising from π – π stacking, thus disfavouring formation of the planar ribbons that would be required for **14** to participate in the cyclic dimer motif **2**. We note that carboxylic acids are also known to participate in interaction motifs other than cyclic dimers, such as

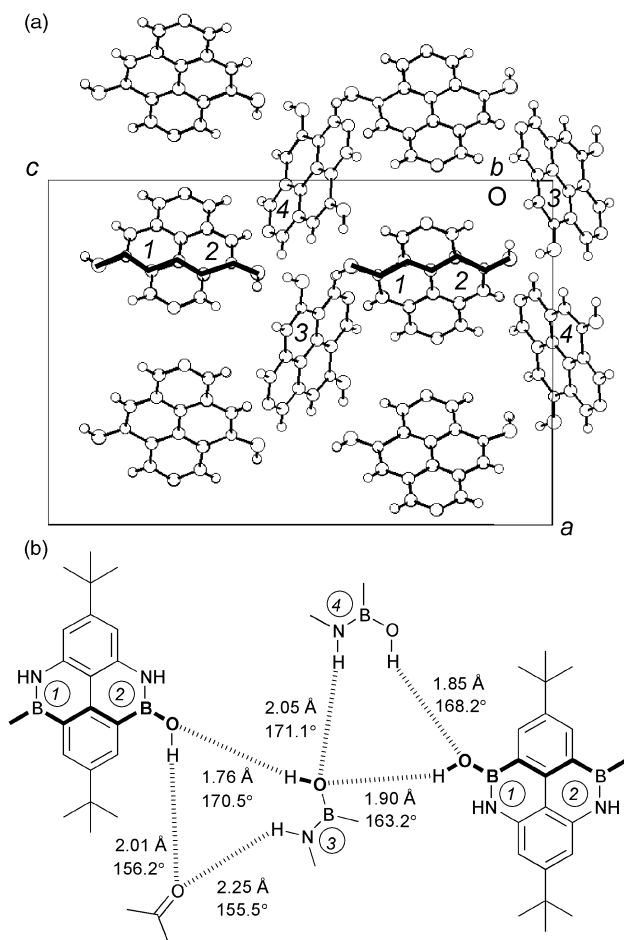


Fig. 5 (a) The crystal structure of $[14_2 \cdot \text{acetone}]$ viewed along the b axis. The *tert*-butyl groups are disordered and have been omitted, together with the acetone molecules, for clarity. The numbers 1 to 4 represent the four crystallographically independent N–B–O functionalities and the bold line represents a chain of molecules linked together by O–H...O(B) hydrogen bonds. (b) A schematic representation of the hydrogen bonding interactions in the crystal structure of $[14_2 \cdot \text{acetone}]$.

chains and expanded rings. Indeed, a recent analysis²³ of the Cambridge Structural Database (CSD, October 1996) suggests that the probability that a molecule bearing a carboxylic acid functionality forms cyclic hydrogen bonded dimers is only about 33%.

It is important to note that the absence of motif **2** from the crystal structure of $[14_2 \cdot \text{acetone}]$ does not necessarily preclude the capability of polymerisation. The recognition sites bring the reaction centres (boron and hydroxy) into close proximity, suggesting that a solid-state transformation may be able to occur at relatively low temperatures.

The first evidence for the solid-state reactivity of the $[14_2 \cdot \text{acetone}]$ co-crystal was the fact that crystalline samples did not melt at temperatures below 400 °C. When a (transparent) single crystal of $[14_2 \cdot \text{acetone}]$ was used for a melting point experiment, the crystal became opaque at 150–160 °C and displayed no further observable change at temperatures up to 400 °C suggesting that some degree of polymerisation had occurred.

The change in the solid-state structure of $[14_2 \cdot \text{acetone}]$ effected by heating was confirmed by variable temperature powder X-ray diffraction studies. When a sample of $[14_2 \cdot \text{acetone}]$ was heated to 100 °C, the powder diffraction peaks became less intense over a period of hours. When the temperature was raised to 160 °C, the diffraction peaks disappeared completely within a matter of minutes. At these temperatures, the sample became amorphous. On subsequently cooling this

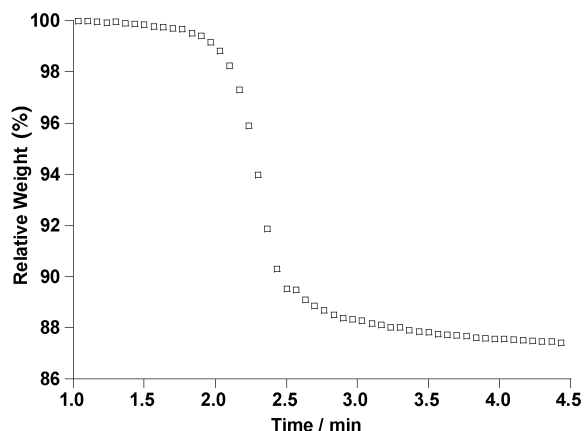


Fig. 6 The mass loss, recorded by thermogravimetric analysis (TGA), on heating a powdered sample of $[14_2 \cdot \text{acetone}]$. The sample was heated from 25 to 300 °C at a rate of 100 °C per minute, after which time (2.75 min) the temperature was held at 300 °C for a further 1.75 minutes.

sample to room temperature, the diffractogram indicated that the sample remained amorphous.

The solid-state chemical reactivity of $[14_2 \cdot \text{acetone}]$ was demonstrated using thermogravimetric analysis (TGA) to measure the loss of mass (water and acetone) from the solid as a consequence of the reaction to give the oligoanhydride **15**. Upon heating from 25 °C to 300 °C (at 100 °C per minute) the total mass loss for powder samples of $[14_2 \cdot \text{acetone}]$ was about 13% (Fig. 6), of which some amount may be attributed to decomposition and sublimation (the theoretical mass loss due to acetone and water is 9.8%). Isothermal TGA measurements of the mass loss suggest that, in keeping with the powder X-ray diffraction studies, the reaction rate is fast at 160 °C and slow at 100 °C (the loss of acetone and water is complete within 30 minutes at 160 °C and within several hours at 100 °C).

In order to confirm that the oligoanhydride **15** had been formed by a solid-state transformation, single crystals of $[14_2 \cdot \text{acetone}]$ were heated at 160 °C for several hours and were then analysed by MALDI-TOF spectrometry. Since the heated crystal had to be dissolved in an appropriate solvent before being applied to a MALDI sample plate, it was crucial to prepare the MALDI samples such that no oligomer condensation occurs in the solution phase. Therefore, MALDI-TOF analysis of a crystal of $[14_2 \cdot \text{acetone}]$ that had not been heated was performed as a control experiment. As a further safeguard, all samples were dissolved in acetone since we have demonstrated that the equilibrium between **14** and **15** in acetone lies on the side of **14**. This solvent ensures that no significant amounts of oligomerisation occur in solution. The MALDI-TOF spectrum of a dilute solution of a crystal of $[14_2 \cdot \text{acetone}]$ in acetone (*ca.* 3 mM) shows the molecular ion 14^+ is the predominant peak (Table 1, entry **D**), but contains no peaks corresponding to the anhydride dimer (**15**, $n = 0$) or larger oligoanhydrides. The spectrum of a heated crystal of $[14_2 \cdot \text{acetone}]$, prepared in an identical manner, shows peaks corresponding to oligoanhydrides up to $n = 7$ (Table 1, entry **E**) confirming that the solid-state transformation yields **15**. Unfortunately, it is impossible to determine the distribution of oligomer lengths in a quantitative manner from the MALDI data, and it is likely that higher oligomer chains, if present, are either not ionised or fragment to form lower oligomers. Interestingly, at a higher laser power setting, peaks corresponding to much larger oligomers are seen ($n = 15+$), although at the same power setting the control sample shows peaks for **15** ($n = 0, 1$), probably arising from aggregation.

Conclusions

We have demonstrated that the unique recognition and reactivity of borazaaromatics can be incorporated success-

fully into bifunctional systems. In solution, the bifunctional borazaaromatic **14** can participate in self-assembly²⁴ mediated by covalent bond formation forming linear oligomers of molecular weight greater than 2000 Da. In the solid-state, the recognition properties of **14** serve to locate the reactive centres in an appropriate orientation for the transformation to form oligomeric species to occur at relatively low temperatures. The positions of the reactive centres within **14** predispose²⁵ the system to form linear oligomers. Studies²⁶ are currently underway in our laboratory to exploit the reactivity of borazaaromatics in systems which are predisposed to form other, more complex, structures.

Experimental

General

Xylene was dried and 1,2-dimethoxyethane was purified by refluxing with sodium and collected by distillation. Et₂O was dried by refluxing with Na–benzophenone and collected by distillation under N₂. All other solvents and reagents were used as received. Dichloroborane–methyl sulfide complex was supplied by Aldrich. Aluminium chloride (powder, ≥99%) and phenyl-dichloroborane (≥98%) were supplied by Fluka. Thin layer chromatography (TLC) was performed on aluminium plates coated with Merck Kieselgel 60 F₂₅₄ and scrutinised under a UV lamp. Column chromatography was performed using Kieselgel 60 (0.040–0.063 mm mesh, Merck 9385) silica. Melting points were determined using an Electrothermal 9200 melting point apparatus and are uncorrected. ¹H NMR spectra were recorded on a Bruker AC300 (300.1 MHz) spectrometer or a Bruker DRX500 (500.1 MHz) spectrometer using the deuterated solvent as the lock and the residual solvent as the internal reference. ¹³C NMR spectra were recorded on a Bruker AC300 (75.5 MHz) spectrometer using the PENDANT sequence. Electron impact mass spectrometry (EIMS) was carried out on a VG PROSPEC mass spectrometer. Liquid secondary ion mass spectrometry (LSIMS) was carried out on a VG ZabSpec mass spectrometer equipped with a caesium ion gun. The sample was dissolved in a small volume of nitrophenyl octyl ether, which had previously been coated onto a stainless steel probe tip. Spectra were recorded in the positive ion mode at a scan speed of 10 s dec⁻¹. Infra-red spectra were recorded (KBr disks) on a Perkin-Elmer Paragon 1000 FTIR spectrometer at ambient temperature. All spectra were recorded at a resolution of 2 cm⁻¹.

Powder X-ray diffractograms were recorded on a Siemens D5005 diffractometer equipped with an Auton Paar HTK 1200 heating stage (operating in reflection mode using Cu-K α radiation). The data were recorded for 2θ in the range 8–40° in steps of 2θ of 0.014° with a counting time of 0.5 seconds per step. Data were recorded at 25 and at 10 °C intervals within the range 100–190 °C. Thermogravimetric analysis (TGA) experiments were performed on a Perkin-Elmer TGA6 instrument using nitrogen as the sample purge gas. Temperature scan experiments were performed using a range of heating rates (20 to 100 °C). Isothermal experiments were performed at temperatures between 100 and 160 °C.

MALDI-TOF mass spectrometry

MALDI-TOF mass spectra were recorded on a Kratos Kompact Maldi III mass spectrometer. A nitrogen laser (337 nm, 85 kW peak laser power, 3 ns pulse width) was used to desorb the sample ions, and the instrument was operated in linear time-of-flight mode with an accelerating potential of 20 kV. A laser power setting of 94 was used for all experiments. Results from 50 laser shots were signal averaged to give one spectrum. An aliquot of matrix (a suspension of cobalt powder in a methanol–glycerol mixture) was deposited on the sample plate surface. After the matrix had dried, a small volume of the

analyte (typically 1 mg dissolved in 1 mL) was layered upon the matrix and allowed to air-dry.

Computational methods

Ab initio quantum mechanical calculations were performed using SPARTAN (Wavefunction, Inc., 18401 Von Karman Suite 370, Irvine, CA 92612, USA, 1998, Version 5.1.1). All atomic coordinates were optimised fully to an RMS gradient of less than 1×10^{-4} au.

Synthetic procedures

4-tert-Butyl-2,6-dinitrobromobenzene 9. 4-tert-Butylbromobenzene (20.0 g, 93.8 mmol) was added dropwise to vigorously stirred fuming nitric acid (*d* 1.5, 50 mL) at 0 ± 5 °C during 30 minutes. The mixture was stirred at 25 °C for one hour and then at 50 °C for 20 minutes after which time the red coloured mixture was poured on to vigorously stirring ice-water (200 mL). The yellow–green precipitate was collected by filtration and washed with water (2×50 mL) and saturated aqueous NaHCO₃ solution (3×50 mL). The solid was dissolved in a mixture of EtOH (200 mL) and acetone (20 mL), with the resulting concentration of the solution under reduced pressure affording the product as pale yellow–green coloured needles (15.18 g, 53%). Mp 129–133 °C (lit.²⁷ 136 °C); ¹H NMR (300 MHz, CDCl₃, 25 °C): δ 7.91 (s, 2H, ArH), 1.37 (s, 9H, CH₃); ¹³C NMR {¹H} (75 MHz, CD₃COCD₃, 25 °C): δ 154.55, 151.56, 124.97, 103.73, 35.65, 30.62; EIMS: *m/z* (relative %): 302 (21) [M]⁺, 304 (20) [M + 2]⁺, 287 (100) [M – CH₃]⁺, 289 (99) [M + 2 – CH₃]⁺.

***p*-tert-Butylbenzeneboronic acid 10.** A solution of 4-tert-butylbromobenzene 21.32 g (100 mmol) in dry Et₂O (100 mL) was added to magnesium turnings and a crystal of iodine. The resulting exotherm maintained the reaction mixture at reflux temperature for several minutes. The resulting ethereal solution of 4-tert-butylphenylmagnesium bromide (100 mmol) was cannulated onto a stirred solution of B(OMe)₃ (10.4 g, 10.0 mmol) in Et₂O (50 mL) during 20 minutes at -76 ± 5 °C under a positive pressure of N₂. The stirred mixture was warmed to 25 °C with stirring overnight and the resulting thick-grey slurry poured onto a 1.84 M aqueous solution of sulfuric acid (60 mL). The aqueous layer was extracted with Et₂O (2×20 mL), the combined extracts dried (MgSO₄), and concentrated under reduced pressure to afford a yellow oil. Addition of Et₂O (*ca.* 5 mL) followed by hexane (*ca.* 30 mL) precipitated the product as white needles (4.7 g). Further crops were obtained by concentration of the mother liquor under reduced pressure followed by the addition of more Et₂O–hexane in the presence of a small quantity of water (total yield 8.30 g, 47%). Mp 200–201 °C (lit.²⁸ (water) 168–170 °C); IR (KBr) *v*: 3332 (O–H) cm⁻¹; ¹H NMR (300 MHz, CD₃COCD₃, 25 °C): δ 7.83 (AA' portion of AA'XX' spin system, ³J(H,H) = 8.2 Hz, 2H, ArH), 7.41 (XX' portion of AA'XX' spin system, ³J(H,H) = 8.2 Hz, 2H, ArH), 7.12 (s, 2H, OH), 1.33 (s, 9H, CH₃); ¹³C NMR {¹H} (75 MHz, CD₃COCD₃, 25 °C): δ 153.98, 135.01, 125.22, 35.28, 21.62; EIMS: *m/z* (relative %): 480 (5) [M₃ – 3H₂O]⁺, 465 (68) [M₃ – 3H₂O – CH₃]⁺, 178 (68) [M]⁺, 163 (100) [M⁺ – CH₃].

2,6-Dinitro-4,4'-di-tert-butylbiphenyl 11. 4-tert-Butyl-2,6-dinitrobromobenzene (3.20 g, 10.56 mmol) was added to a stirred suspension of Pd(PPh₃)₄ (0.416 g, 0.36 mmol, 0.03 mol equiv.) in freshly distilled 1,2-dimethoxyethane (70 mL). After 10 minutes, a solution of *p*-tert-butylbenzeneboronic acid (2.92 g, 16.42 mmol) in EtOH (8 mL) and a solution of Na₂CO₃ (2.55 g, 24 mmol) in water (24 mL) was added and the mixture heated at reflux temperature for 5 hours. Upon cooling, the mixture was filtered through Celite and the filtrate concentrated under reduced pressure to afford an oil dispersed in water which was

added to brine (50 mL) and extracted with Et₂O (2 × 50 mL). The non-aqueous layer was dried (MgSO₄) and the solvent removed under reduced pressure to afford a brown oil. Upon standing, needle-like crystals formed in the oil; these crystals were collected by suction filtration and washed with ethanol to afford the product as grey needles (2.14 g, 57%). Mp 175–177 °C; ¹H NMR (300 MHz, CDCl₃): δ 7.93 (s, 2H, ArH), 7.42 (d, ³J(H,H) = 8.4 Hz, 2H, ArH), 7.17 (d, ³J(H,H) = 8.4 Hz, 2H, ArH), 1.42 (s, 9H, CH₃), 1.33 (s, 9H, CH₃); ¹³C NMR {¹H} (75 MHz, CDCl₃): δ 153.96, 152.38, 151.04, 127.90, 127.61, 127.22, 125.86, 123.66, 35.67, 34.87, 31.38, 30.95; EIMS: *m/z* (relative %): 356 [M]⁺ (12), 341 (100) [M – CH₃]⁺. Anal. Calcd for C₂₀H₂₄N₂O₄: C, 67.58; H, 6.77; N, 7.92. Found: C, 67.40; H, 6.79; N, 7.86%.

2,6-Diamino-4,4'-di-*tert*-butylbiphenyl 12. 2,6-Dinitro-4,4'-di-*tert*-butylbiphenyl (1.90 g, 5.33 mmol) was added to a mixture of palladium on carbon (5%, 563 mg, 5 mol%) and EtOAc (50 mL) and the mixture degassed under reduced pressure. Hydrogen gas was introduced *via* a balloon and the mixture was stirred for 24 hours after which time it was filtered through a pad of Celite. The red coloured filtrate was evaporated to dryness under reduced pressure and the solid residue dissolved in CH₂Cl₂ (*ca.* 5 mL). Trituration with hexane (*ca.* 20 mL) afforded **12** as a light-orange powder (1.32 g, 84%). Mp 212–214 °C; IR (KBr) *v*: 3434 (N–H), 3420 (N–H), 3343 (N–H) cm⁻¹; ¹H NMR (300 MHz, CD₃COCD₃, 25 °C): δ 7.53 (d, ³J(H,H) = 8.5 Hz, 2H, ArH), 7.23 (d, ³J(H,H) = 8.5 Hz, 2H, ArH), 6.21 (s, 2H, ArH), 3.81 (s, 4H, NH₂), 1.35 (s, 9H, CH₃), 1.24 (s, 9H, CH₃); ¹³C NMR {¹H} (75 MHz, CD₃COCD₃, 25 °C): δ 151.75, 150.42, 145.97, 134.48, 131.10, 126.95, 111.16, 102.84, 35.01, 34.68, 31.61; EIMS: *m/z* (relative %): 296 (100) [M]⁺ (100), 281 (42) [M – CH₃]⁺. HRMS. Calcd. for C₂₀H₂₈N₂ [M]⁺: 296.2253. Found: 296.2255.

2,7-Di-*tert*-butyl-5,9-diphenyl-5,9-dibora-4,10-diazapyrene-4,10-dium-5,9-diide 13. Dichlorophenylborane (318 mg, 2 mmol) was added in small portions to a solution of the diamine **12** (296 mg, 1 mmol) in dry xylene. The stirred mixture was heated at reflux temperature for 90 minutes, cooled, and AlCl₃ (27 mg, 0.2 mmol) added. The mixture was refluxed for 15 hours, cooled, additional AlCl₃ added (27 mg, 0.2 mmol) and the mixture refluxed for a further 4 hours. Standard aqueous workup followed by column chromatography (SiO₂, CH₂Cl₂ : hexane, 4 : 1, *v/v*) afforded the product as an off-white foamy solid (102 mg, 22%). Mp 289–291 °C; IR (KBr) *v*: 3368 (N–H) cm⁻¹; ¹H NMR (300 MHz, CDCl₃, 25 °C): δ 8.67 (s, 2H, ArH), 7.94–7.91 (m, 6H), 7.60–7.50 (m, 6H), 7.17 (s, 2H, ArH), 1.46 (s, 9H, CH₃), 1.44 (s, 9H, CH₃); ¹³C NMR {¹H} (75 MHz, CDCl₃, 25 °C): δ 151.2, 146.8, 139.4, 139.2, 135.6, 133.5, 128.8, 128.3, 111.5, 108.0, 35.1, 35.0, 31.8, 31.7; EIMS: *m/z* (relative %): 468 (100) [M]⁺, 453 (77) [M – CH₃]⁺. HRMS. Calcd for C₃₂H₃₅B₂N₂ [M + H]⁺: 469.2986. Found: 469.3002.

2,7-Di-*tert*-butyl-5,9-dihydroxy-5,9-dibora-4,10-diazapyrene-4,10-dium-5,9-diide 14. Dichloroborane–dimethyl sulfide complex (943 mg, 6.51 mmol) was added in small portions to a solution of the diamine **12** (643 mg, 2.17 mmol) in dry xylene. The stirred mixture was heated at reflux temperature for 2 hours, cooled, AlCl₃ (87 mg, 0.3 mmol) added and the mixture heated at reflux temperature for a further 18 hours. The mixture was washed with water, before addition of hexane to the organic phase which precipitated **15** as a white powder (546 mg, 1.57 mmol, 72%, based upon molecular weight of **14**). Recrystallisation of this powder by slow diffusion of hexane into a solution of **15** in a mixture of hexane and acetone gave colourless crystals of [**14**·acetone]. *Spectroscopic data* for [**14**·acetone]: Mp >400 °C (transforms into **15** at temperatures >100 °C); IR (KBr) *v*: 3529–3184 (several absorptions, O–H and N–H) cm⁻¹; ¹H NMR (300 MHz, CD₃COCD₃, 25 °C): δ 8.55 (s,

2H, C(6)H and C(8)H), 7.68 (s, 2H, NH), 7.26 (s, 2H, OH), 6.96 (s, 2H, C(3)H and C(11)H), 1.45 (s, 9H, C(7)(CH₃)₃), 1.36 (s, 9H, C(2)(CH₃)₃); ¹³C NMR {¹H} (75 MHz, CD₃COCD₃, 25 °C): δ 151.4, 146.5, 143.0, 141.8, 141.7, 131.4, 106.1, 35.4, 35.1, 32.0, 31.8; LSIMS: *m/z* (relative %): 348 (37) [M]⁺, 252 (100).

2,7-Di-*tert*-butyl-5,9-dimethoxy-5,9-dibora-4,10-diazapyrene-4,10-dium-5,9-diide 16. Solutions of **14** and **15** in methanol gave **16** *in situ*, which precipitated as colourless rhombic crystals either upon standing for hours or immediately if the solution is sufficiently concentrated. Mp 330.5–333.5 °C; EIMS: *m/z* (relative %): 376 (100) [M]⁺, 361 (75) [M – 15]⁺. Neither ¹H NMR nor ¹³C NMR spectra could be obtained since **16** is almost insoluble in CD₃OD. NMR spectra could not be recorded in other solvents since **16** is hydrolysed readily to **14**.

Acknowledgements

This research was supported by the University of Birmingham and the Engineering and Physical Sciences Research Council (Quota award to JMAR and Postdoctoral Fellowship to BMK).

References

- For general reviews of solid-state organic reactions, see G. M. J. Schmidt, *Pure Appl. Chem.*, 1971, **27**, 657; J. M. Thomas, *Philos. Trans. R. Soc. London*, 1974, **277**, 251; V. Ramamurthy and K. Venkatesan, *Chem. Rev.*, 1987, **87**, 433; F. Toda, *Synlett*, 1993, 303; N. B. Singh, R. J. Singh and N. P. Singh, *Tetrahedron*, 1994, **50**, 6441; J. R. Scheffer and C. Scott, *Science*, 2001, **291**, 1712.
- K. S. Feldman and R. F. Campbell, *J. Org. Chem.*, 1995, **60**, 1924.
- G. W. Coates, A. R. Dunn, L. M. Henling, J. W. Ziller, E. B. Lobkovsky and R. H. Grubbs, *J. Am. Chem. Soc.*, 1998, **120**, 3641.
- G. W. Coates, A. R. Dunn, L. M. Henling, D. A. Dougherty and R. H. Grubbs, *Angew. Chem., Int. Ed. Engl.*, 1997, **36**, 248.
- G. R. Desiraju, *Solid-state Ionics*, 1997, **101**, 839.
- For general reviews of borazaaromatics and related compounds, see P. M. Maitlis, *Chem Rev.*, 1962, **62**, 223; M. J. S. Dewar, *Prog. Boron Chem.*, 1964, **1**, 235.
- For a recent discussion of the term “supramolecular synthon”, see A. Nangia and G. R. Desiraju, *Top. Curr. Chem.*, 1998, **198**, 57.
- J. M. A. Robison, B. M. Kariuki, D. Philp and K. D. M. Harris, *Tetrahedron Lett.*, 1997, **38**, 6281.
- K. D. M. Harris, B. M. Kariuki, C. Lambropoulos, D. Philp and J. M. A. Robison, *Tetrahedron*, 1997, **53**, 8599.
- M. C. Etter, *Acc. Chem. Res.*, 1990, **23**, 120; M. C. Etter, J. C. Macdonald and J. Bernstein, *Acta Crystallogr., Sect. B*, 1990, **46**, 256.
- R. Alcalá and S. Martínez-Carrera, *Acta Crystallogr., Sect. B*, 1972, **28**, 1671.
- J. Yang, J.-L. Marendaz, S. J. Geib and A. D. Hamilton, *Tetrahedron*, 1994, **35**, 3665.
- D. J. Duchamp and R. E. Marsh, *Acta Crystallogr., Sect. B*, 1969, **25**, 5.
- S. V. Kolotuchin, E. E. Fenlon, S. R. Wilson, C. J. Loweth and S. C. Zimmerman, *Angew. Chem., Int. Ed. Engl.*, 1995, **34**, 2654.
- There is literature precedent for the synthesis of a borazapyrene (5,9-diphenyl-5,9-dibora-4,10-diazapyrene-4,10-dium-5,9-diide): S. S. Chissick, M. J. S. Dewar and P. M. Maitlis, *Tetrahedron Lett.*, 1960, **23**, 8.
- J. Cornforth, A. F. Sierakowski and T. W. Wallace, *J. Chem. Soc., Perkin Trans. 1*, 1982, 2299.
- N. Miyarua and A. Suzuki, *Chem Rev.*, 1995, **95**, 2457.
- M. J. S. Dewar, R. B. K. Dewar and Z. L. F. Gaibel, *Org. Synth. Coll. Vol.*, 1973, **5**, 727.
- Crystal data* for **16** at 294(2) K: [C₂₂H₃₀B₂N₂O₅], *M* = 376.10 g mol⁻¹, monoclinic, space group *C2/m*, *a* = 10.997(2), *b* = 7.012(2), *c* = 14.878(4) Å, β = 106.331(14)°, *V* = 1101.0(5) Å³, *Z* = 2, *D_c* = 1.134 g cm⁻³, λ = 0.71069 Å, *F*(000) = 404. A colourless plate-like crystal of dimensions 0.3 mm × 0.2 mm × 0.1 mm was used. Data were measured on a Rigaku R-AXIS II rotating anode X-ray diffractometer using graphite-monochromated Mo-Kα radiation. In total, 1047 unique reflections were measured (5.70° ≤ 2θ ≤ 51.30°, *R*_{int} = 0.058) of which 655 were considered to be observed. The structure was solved by direct methods (SHELXS86, G. M. Sheldrick, University of Göttingen, Germany, 1986) and

- non-hydrogen atom positions were refined (SHELXL93, G. M. Sheldrick, University of Göttingen, Germany, 1993) with anisotropic displacement parameters by full-matrix least squares to give $R = 0.068$, $wR_2 = 0.194$. Crystallographic data (excluding structure factors) for this structure have been deposited with the Cambridge Crystallographic Data Centre, CCDC 165970. See <http://www.rsc.org/suppdata/p2/b1/b104794a/> for crystallographic files in .cif or other electronic format.
- 20 The four resonances in the aromatic region of the ^1H NMR spectrum of **14** in d_6 -acetone were assigned by NOE experiments which were dependent on the identification of the (exchangeable) resonance arising from the OH proton. Addition of D_2O to the sample resulted in the disappearance of the resonance at δ 7.25, and this resonance was thus assigned as the OH proton.
- 21 *Crystal data* for [**14** $_2$ ·acetone] at 296(2) K: $[(\text{C}_{25}\text{H}_{26}\text{B}_2\text{N}_2\text{O}_2)_2 \cdot \text{C}_3\text{H}_6\text{O}]$, $M = 754.18 \text{ g mol}^{-1}$, orthorhombic, space group $Pca2_1$, $a = 16.598(2)$, $b = 11.1270(12)$, $c = 24.240(3) \text{ \AA}$, $V = 4476.8(8) \text{ \AA}^3$, $Z = 4$, $D_c = 1.119 \text{ g cm}^{-3}$, $\lambda = 0.71069 \text{ \AA}$, $F(000) = 1616$. A colourless block-like crystal of dimensions $0.5 \text{ mm} \times 0.3 \text{ mm} \times 0.2 \text{ mm}$ was used. Data were measured as described for **16**; 8190 unique reflections were measured ($3.36^\circ \leq 2\theta \leq 51.38^\circ$, $R_{\text{int}} = 0.067$) of which 7860 were considered to be observed. Structure solution and refinement as described for **16** gave $R = 0.056$, $wR_2 = 0.128$. Given the unusual bonding in this system, the N–H and O–H distances were not normalised using standard distances; rather, these distances were normalised according to the optimised HF/6-31G geometry of **7** (N–H and O–H distances 1.00 and 0.94 Å respectively). Crystallographic data (excluding structure factors) for this structure have been deposited with the Cambridge Crystallographic Data Centre, CCDC 165969. See <http://www.rsc.org/suppdata/p2/b1/b104794a/> for crystallographic files in .cif or other electronic format.
- 22 G. A. Jeffrey, *An Introduction to Hydrogen Bonding*, Oxford University Press, New York, 1997, pp. 98–107.
- 23 F. H. Allen, W. D. S. Motherwell, P. R. Raithby, G. P. Shields and R. Taylor, *New J. Chem.*, 1999, 25.
- 24 D. Philp and J. F. Stoddart, *Angew. Chem., Int. Ed. Engl.*, 1996, **35**, 1154; D. S. Lawrence, T. Jiang and M. Levett, *Chem. Rev.*, 1995, **95**, 2229; J. S. Lindsey, *New J. Chem.*, 1991, **15**, 153; G. M. Whitesides, J. P. Mathias and C. T. Seto, *Science*, 1991, **254**, 1312.
- 25 For examples of covalent self-assembly, see S. J. Rowan, P. A. Brady and J. K. M. Sanders, *Angew. Chem., Int. Ed. Engl.*, 1996, **35**, 2143; P. A. Brady and J. K. M. Sanders, *Chem. Soc. Rev.*, 1997, **26**, 327; S. J. Rowan and J. K. M. Sanders, *J. Org. Chem.*, 1998, **63**, 1536; J. Ipaktschi, R. Hosseinzadeh and P. Schlaf, *Angew. Chem., Int. Ed.*, 1999, **38**, 1658.
- 26 P. J. Comina, D. Philp, B. M. Kariuki and K. D. M. Harris, *Chem. Commun.*, 1999, 2279.
- 27 I. Boedtker, *Bull. Soc. Chim. Fr.*, 1906, **35**, 830.
- 28 K. S. Chan, X. Zhou, M. T. Au and C. Y. Tam, *Tetrahedron*, 1995, **51**, 3129.